Physical Science International Journal

17(4): 1-14, 2018; Article no.PSIJ.39318
ISSN: 2348-0130

Thermal Behaviour of Bone Cement in Hip Replacement

J. U. Ikekwem[1], J. L. Chukwuneke[1*] and S. N. Omenyi[1]

[1]Department of Mechanical Engineering, Nnamdi Azikiwe University, Awka, Nigeria.

Authors' contributions

This work was carried out in collaboration between all authors. All authors read and approved the final manuscript.

Article Information

DOI: 10.9734/PSIJ/2018/39318
Editor(s):
(1) Pratima Parashar Pandey, Professor, Polymer Composites, Nanotechnology Applied Sciences, College of Engineering & Technology, Integrated Institutes of Learning, Dr. APJ Abdul Kalam Technical University, Greater Noida, India.
(2) Christian Brosseau, Distinguished Professor, Department of Physics, Université de Bretagne Occidentale, France.
Reviewers:
(1) Hajime Yamanaka, National Hospital Organization, Shimoshizu Hospital, Japan.
(2) Triki Mohamed Amine, Sahloul Hospital, University of Sousse, Tunisia.
(3) Hiroaki Kijima, Akita University Graduate school of Medicine, Japan.
Complete Peer review History: http://www.sciencedomain.org/review-history/23770

Original Research Article

Received 13th December 2017
Accepted 26th February 2018
Published 22nd March 2018

ABSTRACT

This work involved the study of heat transfer in a cemented hip replacement. The recent rise in cemented hip replacement in Orthopaedic and trauma surgery is of alarming concern to the material usage and conditions it been subjected to. Bone cementing which is the main technology providing the bonding mechanism between the femur cavity and the prosthesis stem is the polymerization reaction between the powder and liquid monomer which is an exothermic reaction. This heat transfer mechanisms between the bone cement, the prosthesis stem and the femur bone is of concern to biomechanics engineers. The ANSYS 15.0 software was used in conjunction with the Autodesk software to model the scenario and simulate it using steady state thermal-structural analysis. It was found that the temperature that resulted from the exothermic reaction of the PMMA polymer (used as bone cement) raised the temperature in the assembly creating a heat flux amounting to $5.11x10^{-7}W/m^2$ in which only $2.83x10^{-7}$ W/m^2 got to the femur bone while the rest was absorbed by the prosthesis stem and the femur bone. The specific heat capacities of PMMA and femur bone were calculated as1.297kJ/kg.K and 0.59kJ/kg.K respectively. The Young Modulus for PMMA was found as 28.78GPa and 18.79GPa for femur bone. These show that it is possible to determine these properties from the simulation studies.

**Corresponding author: E-mail: jl.chukwuneke@unizik.edu.ng;*

Keywords: Heat transfer; femur bone; prosthesis stem; thermal-structural analysis; specific heat capacity; bone cementing.

1. INTRODUCTION

Bone cementing over the years has been very successfully used in providing aid for artificial joints such as shoulder, hip joints, knee joints, and elbow joints for more than half a century. This technology which is newly introduced in Nigeria has indigenous companies trying to work out the suitable local materials that can be engaged in bone cementing that is comparable to the imported counterpart [1]. Artificial joints like the hip joints are usually anchored by bone cementing which is meant to fill the free space that would exist between the prosthesis and the bone. Hence it plays a vital role in creating an elastic limit or zone due to thermal loads agitated by external effects such as walking, running, sitting and even body weights [2]. This is essential because the human hip is acted on by approximately 10–12 times the body weight and therefore the bone cement must be able to contain the forces acting on the hips by absorbing the forces and pressures at the contact segment to ensure that the artificial implant remains in place over the long term [3]. Bone cement chemically is nothing more than Plexiglas (polymethylmethacrylate "PMMA"). PMMA was clinically used the first time in 1940 in plastic surgery to fill up the gaps in the skull. Comprehensive clinical tests of the compatibility of bone cements with the body were conducted before their use in surgery. The excellent tissue compatibility of PMMA allowed it to be used as bone cement for anchorage of head prostheses in the 1950s [4].

Charnley after experimenting with various materials while working at Manchester University, eventually settled on PMMA -a viscous dough which he formed by mixing the powder with the liquid monomer [5]. In 1958, he performed his first case in Manchester. Charnley was the first to apprehend that PMMA could be easily used to fill the medullar canal and merge with the bone morphology. The cement acted to increase the biomechanical stability and decrease the stress on the implant and he settled on the idea of using cement as a 'grout' for the hip implants [5]. Despite all the early scepticism, PMMA is being used as bone cement for implant fixation in various Orthopaedic and trauma surgeries to this day.

There exist some external problematic factors that lead to adverse effects of bone cementing. With different loadings acting on the joint such as body weight, walking and running, the internal friction increases thereby increasing the internal temperature of the cemented bone. This leads to an obstruct expansion of the cemented bone above the elastic zone and hence causes aseptic loosening [6].

Additionally, this problem is based on incomplete heat transfer in the bone-cement-prosthesis system. It is believed that mechanical properties of the cement and thermal cum chemical injuries of the bone tissue in the bone-cement interface are two main factors that affect the heat transfer process in the system [7].

Even though the practices and availability of various types of bone cement have greatly progressed over the past century, further research still continues to develop more clinical applications and to reduce the adverse effects associated with their usage. The aim of this research is to study the heat transfer on a cemented hip replacement joint.

2. THEORETICAL CONCEPTS

2.1 The Governing Equations

The heat-flux equation is the energy balance for heat conduction through an infinitesimal non-moving volume. The energy balance equation applied to a system of finite volume [8]:

$$\left.\frac{dH}{dt}\right|_p = \dot{Q} \quad \rightarrow \quad \int_V \rho c \frac{\partial T}{\partial t} dV = -\int_A \vec{\dot{q}} \cdot \vec{n} dA + \int_V \phi dV \tag{1}$$

Where $\dot{Q}$ is some energy released per unit volume (by chemical reactions), sometimes written as $\dot{q}_{gen}$. Eq.(1) can be read as "the time-increment of enthalpy within the volume due to the heat input through the frontier plus the energy dissipation in the interior"; the minus sign coming from the choice of $\vec{n}$ as the normal outwards vector. When the Gauss-Ostrogradski theorem of vector calculus is used to transform the area-integral to the volume-integral Eq.(1) becomes [8]:

$$\int_V \rho c \frac{\partial T}{\partial t} dV = -\int_A \vec{q} \cdot \vec{n} dA + \int_V \phi dV = -\int_V \nabla \cdot \vec{q}\, dV + \int_V \phi dV \quad \rightarrow$$
$$\xrightarrow{V \to 0} \quad \rho c \frac{\partial T}{\partial t} = -\nabla \cdot \vec{q} + \phi \qquad (2)$$

To solve this numerically by the finite element method, we multiply Eq.(2) by a weighting function $v(x)$, and then set the total weighted residual error to zero [9].

$$\int_\Omega \upsilon p C_p \frac{\partial T}{\partial t} d\Omega - \int_\Omega \upsilon \nabla . (k \upsilon T)\, d\upsilon = 0 \qquad (3)$$

Using the symmetry of $\nabla \cdot (vk \nabla T)$, we have

$$\upsilon \nabla . (k \nabla T) = \nabla . (\upsilon k \nabla T) - k \nabla T . \nabla \upsilon. \qquad (4)$$

Substituting Eq.(3) into Eq.(4) and using the divergence theorem;

$$\int_\Omega \upsilon p C_p \frac{\partial T}{\partial t} d\Omega + \int_\Omega k \nabla T . \nabla \upsilon d\Omega = \int_{\partial\Omega} \upsilon k \frac{\partial T}{\partial n} ds. \qquad (5)$$

Imposing the boundary conditions into Eq.(5) yields;

$$\int_\Omega \upsilon p C_p \frac{\partial T}{\partial t} d\Omega + \int_\Omega k \nabla T . \nabla \upsilon d\Omega + \int_{\partial\Omega} \upsilon h \infty T ds. = \int_{\partial\Omega} \upsilon h \infty T_{ext} ds. \qquad (6)$$

Therefore, the variation statement for the boundary value problem can be stated as follows [9]:

Find $T = T(x, t) \in H1(\Omega)$ such that for every $t \in I$

$$(T_t, \upsilon) + a(T, \upsilon) = L(\upsilon) \ \forall \upsilon \in H_0^1(\Omega) \qquad (7)$$

Where; $(T_t, \upsilon) + a(T, \upsilon) = L(\upsilon) \ \forall \upsilon \in H_0^1(\Omega)$

$$T(x, 0) = \hat{T}(x)$$

$$(T\ \upsilon) \ = \ \int_\Omega \upsilon p C_p \frac{\partial T}{\partial t} d\Omega.$$

Let $H^1h(\Omega)$ be a finite dimensional subspace of H^1 with basic functions $\{\phi 1, \phi 2, \ldots, \phi n\}$. Then, the variation problem is approximated by:

Find $Th(x, t) \in H^1h$ such that
$Th(x, 0) = \hat{} T(x)$ and

$$\left(\frac{\partial T_h}{\partial t}, \upsilon h \right) + a\left(T_h, \upsilon_h\right) = L(\upsilon_h), \forall \upsilon_h \in H_h^I. \qquad (8)$$

In the usual way, we introduce a discretization of Ω as a union of elements Ω*e*, i.e, $\Omega \longrightarrow \cup Ee = 1 \Omega e$ and approximate $T(x, t)$ at t by:

$$T = \sum_{j=1}^{N} \phi_j T_j, \ \upsilon = \sum_{j=1}^{N} \phi_j \upsilon_j \qquad (9)$$

2.2 Femur Design

For the prosthesis stem which is inserted into the femur bone, it is essential to dimensionally design each component of the hip replacement for determining the heat transfer characteristics. The prosthesis stem spans 155.5 mm long, with a ball of 36 mm in diameter. The stem exhibits 3 diametric segments. The topmost stem is 20.96 mm, the second segment is 17.79 mm and the bottom segment of the stem is 14.31 mm (see Fig. 1). This is because of the non-uniformity of the femur hip and for the easy of insertion and removal of the prosthesis stem.

The femur design was accomplished using the Autodesk Inventor software. The top section bone was designed with a diameter of 30.91mm while the bottom section was 21 mm in diameter; a cavity bored using the cut extrude function was made having a diametric hole of the top section of 18.81 mm while the bottom section of the cavity was 20 mm. The gap between the femur and the cavity gives the allowance for the bone cementing operation (see Fig. 2). The bone spans a length of about 200 mm which was considered from the design standard.

2.3 Experimentation

2.3.1 Materials and material properties

PMMA used in this study as the bone cement as two main components: the powder and the liquid. The densities of both components have been reported in the literature [10] as about 1100 kg/m^3 but in order to simplify the model, the material properties of the final PMMA mixture are considered. The mass density of the bone cement mixture is assumed to be constant 1.1×10^{-6} kg/mm^3 as proposed by Baliga et al. [11]. According to Perez et al. [12], the specific heat of bone cement c is reported to be either temperature dependent $c = 1.25 \times 10^3 + 6.5T$J/kg^{o}C or constant varying between 1450 and 2000J/kg^{o}C. The thermal conductivity value, k Cement, is assumed to be constant, 0.0002W/mm◦C [12]. Bone cement material properties change depending on the

polymerization process involved and the modulus of elasticity E which is time-dependent. Experimental studies [12–13] on the modulus of elasticity of the fully solidified cement have reported a wide range of values: 1583–4120MPa. In the present model, an average value of 2400MPa was assumed. The first important new assumption in the numerical model proposed here is the consideration of the modulus of elasticity (E) of the PMMA mixture as a function of the modulus of elasticity of the fully solidified cement (E solidified) and its polymerization fraction p.

The prosthesis stem however, is materialized based on the Metal on Metal (MOM) formation. Both the socket and the ball are made of either stainless steel, titanium, chromium, cobalt or some combination of these. For this study, titanium is used.

PMMA has high mechanical strength, high Young's Modulus and low elongation. It does not shatter on rupture. It is one of the hardest thermoplastics and is also highly scratch resistant. It exhibits low moisture and water absorbing capacity, which confers on its products good dimensional stability. Both of these characteristics increase as the temperature rises. Tables 1 and 2 show some of the mechanical and thermal characteristics of PMMA.

The thermal stability of standard PMMA is only 65^{o}C. Its resistance to temperature changes is very good.

Table 1. Physical properties of PMMA [14]

Physical properties	Value
Density	1.15 - 1.19 g/cm3
Linear Mould Shrinkage	0.003 - 0.0065 cm/cm
Melt Flow	0.9 – 27 g/10 min

Titanium is a chemical element with symbol Ti and atomic number 22. It is a lustrous transition metal with a silver colour, low density, and high strength (Table 3). Titanium is resistant to corrosion in sea water, aqua regia, and chlorine. The two most useful properties of the metal are corrosion resistance and strength-to-density ratio, the highest of any metallic element. In its unalloyed condition, Titanium is as strong as some steels, but less dense.

Bone naturally is brittle in nature. The strength of natural bone varies considerably by type, composition and age. The compressive strength of the strong outer (cortical) bone of a thighbone (femur) is typically about 150 MPa, while the spongier inner bone can exhibit a compressive strength below 10 MPa. In Table 3, typical mechanical property values of an entire human thighbone are given. For the bone, the following properties of density, Young's Modulus and Poisson's Ratio are used as 2000 Kg/m^3, 2.130 GPa and 0.3 respectively for analysis [15].

The thermal conductivity varies also depending on the dryness of the bone. The wet bone has about four times the thermal conductivity of the

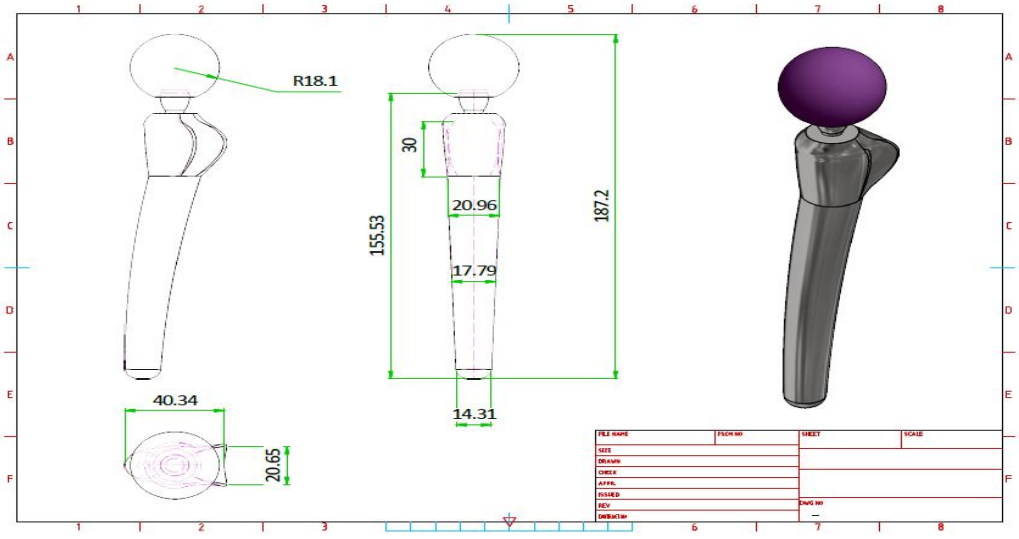

Fig. 1. Isometric and orthographic drawing of the prosthesis stem

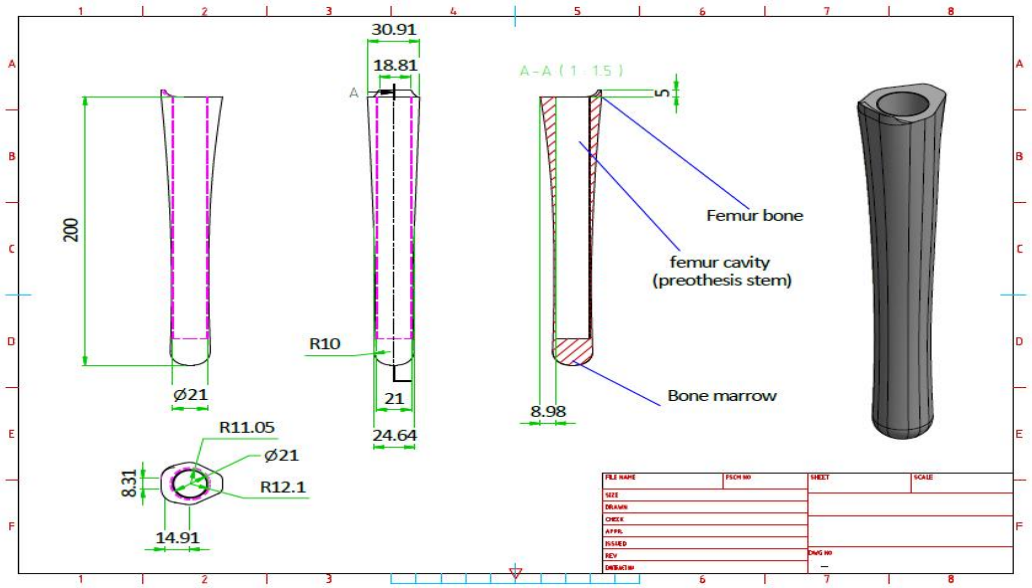

Fig. 2. Isometric and orthographic drawing of the femur bone

Table 2. Mechanical and thermal properties of PMMA [14]

(a) Mechanical properties of PMMA		(b) Thermal properties of PMMA	
Mechanical Properties	**Value**	**Thermal Properties**	**Value**
Hardness, Rockwell M	63 – 97	Specific Heat Capacity	1.46 - 1.47 J/g.°C
Tensile Strength, Ultimate	47 - 79 MPa	Thermal Conductivity	0.19 - 0.24 W/m.K
Elongation at Break	1 - 30 %	Maximum Service Temperature, Air	41 -103 °C
Tensile Modulus	2.2 - 3.8 GPa	Melting Point	130°C

dry done. The conductivity is found to be 0.58±0.018 W/m.K in the longitudinal direction, 0.53±0.030 W/m.K in the circumferential direction, and 0.54±0.020 W/m.K in the radial direction. Because the directional variations are small, it is concluded that bovine cortical bone can be treated as thermally isotropic [15].

2.3.2 Experiment

The only experiment done was in the mixing of the cement to determine the appropriate temperature for the simulation studies. PMMA bone cement preparation involves mixing the solid component, powder, with the liquid component. The ratio is usually 2g of powder to 1ml of liquid; however, this composition can vary depending on the type of cement used. Usually the solid part is the polymer, PMMA, plus the initiator, benzoyl peroxide, and the liquid part is the pure monomer, Methyl methacrylate (MMA), plus the activator. During the polymerization process, monomer MMA is converted into PMMA, which involves an exothermic reaction. Mixing together the powder and the liquid components marks the start of the polymerization process. During the reaction, the cement viscosity increases, slowly at first, then later more rapidly. Studies have shown that high viscosity cements result in better prosthetic fixation, as compared to low viscosity cements. Immediately after mixing, a thermocouple was placed on the bone cement to determine the temperature.

The set up used for this purpose is shown in Fig. 3. The mixing of the bone cement performed in the ambient temperature of 25°C was repeated seven times within the temperature range 43°C to 47°C at time frame of 160s. The values of maximum temperature and time for each experiment were recorded on Table 3.

Table 3. Properties of titanium and human femur bone [15]

(a) Properties of titanium		(b) Properties of human	
Properties	**Value**	**Properties**	**Thighbone (Femur)**
Thermal Expansion	8.6 µm/(m·K) (25 °C)	Density, g/cm^3	1.6 – 1.7
Thermal Conductivity	21.9 W/(m·K)	Young's Modulus, GPa	10 – 15
Young's Modulus	116 GPa	Tensile Strength, MPa	90 – 130
Shear Modulus	44 GPa	Compressive Stress, MPa	130 – 200
Bulk Modulus	110 GPa	Fracture Strain, %	1 – 3
Poisson Ratio	0.32	Toughness, MPa.m$^{1/2}$	1 – 2
		Hardness (Vickers)	50 – 100

This temperature range is within the range of values reported in the literature [15]. Swenson et al. [16], recorded that the maximum temperature attained during polymerisation ranged from 60°C to70°C. Homsy et al. [17], reported a peak temperature of 60°C and 70°C of the bone cement. Noble [18], reported that the maximum temperature attained during polymerization ranged from 60°C to 70°C for seven cements tested.

Table 4. Values of the recorded temperature

Experimental no.	Maximum temperature (°C)	Time (s)
1	45	105
2	47	160
3	44.4	100
4	46.5	158
5	47	155
6	46.7	159
7	47	157

Since physical experiment using human femur was not performed, the results of the temperature values in Table 4 were used for simulation studies only.

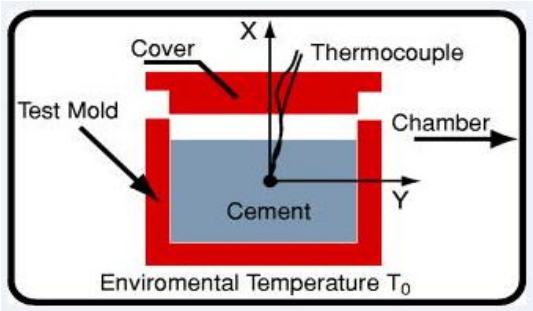

Fig. 3. Experimental set-up

3. RESULTS AND DISCUSSION

3.1 Model Analysis

At this phase, the finite element analysis (FEA) was performed on the femur bone to simulate the thermal behaviour as the bone cement was visualized placed alongside the prosthesis stem of the femur cavity. The Ansys software was deployed alongside with the Autodesk Inventor through a computer aided Engineering to efficiently and effectively simulate the whole process. After the importation of the assembled model, the physical and mechanical properties of the materials, PMMA, Titanium, prosthesis stem and the bone structure, as defined in Tables 1 to 3 were used.

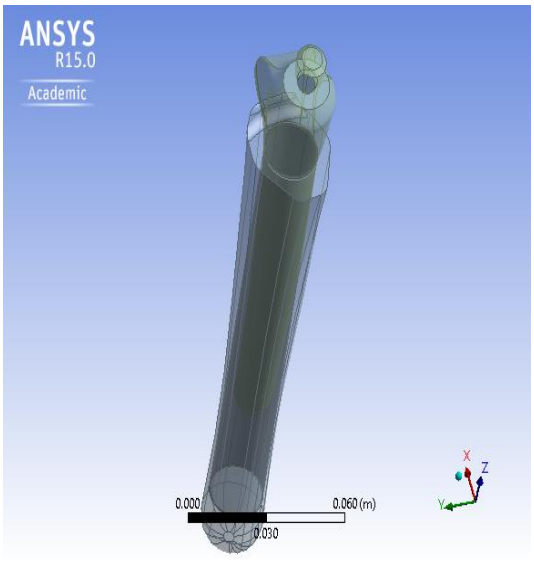

Fig. 4. Assembled geometry for Mesh preparation

3.2 Model Preparation

The geometry was modelled using the Ansys software. The co-ordinates were set to locate the axis and origin of the geometry. Since the geometry consists of no movable parts, the contacts areas were set as fixed (Fig. 4).

After this, the model was discretized into finite elements. The discretization reduced the model into smaller elements with nodes. For a discreet setting, the meshing process took the tetrahedral elemental structure. This element accommodated the processing of 3D models in which the x, y and z-axes were considered in the setting of the boundary conditions and the acknowledgment of their effects. Fig.5 is the meshed geometry showing the nodes and elements of the assembled bone. The total elements and nodes recorded were 20545 and 127247 respectively (Table 5).

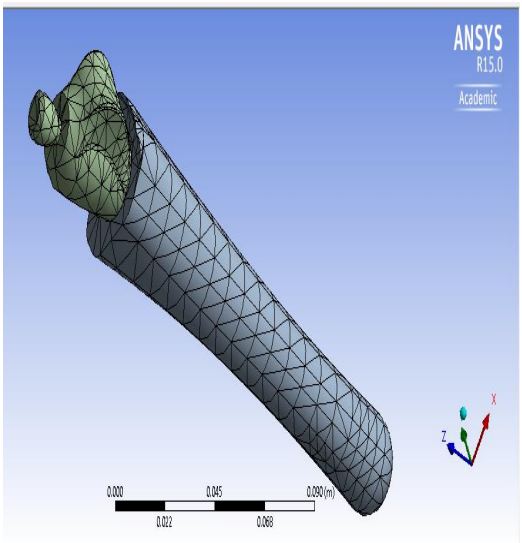

Fig. 5. Meshing of the assembled Model

A finite element model of the bone cemented joint was produced using the Computer Aided Engineering (CAE) package, ANSYSv15.0. The precision and accuracy of the model depends upon its element size or number of nodes and time step size. The increase in number of nodes not only increases the accuracy of the model, but also increases the processing time of the model. An optimum solution could be reached by increasing node density near the region of high-temperature gradient, which is in the vicinity of weld line, and decreasing node density near the region of low-temperature gradient, which is away from the weld line

Table 5. Mesh configurations

Object Name	*Mesh*
State	Solved
Defaults	
Physics Preference	Mechanical
Relevance	0
Sizing	
Use Advanced Size Function	Off
Relevance Center	Coarse
Element Size	Default
Initial Size Seed	Active Assembly
Smoothing	Medium
Transition	Fast
Span Angle Center	Coarse
Minimum Edge Length	1.5556e-004 m
Inflation	
Use Automatic Inflation	None
Inflation Option	Smooth Transition
Transition Ratio	0.272
Maximum Layers	5
Growth Rate	1.2
Inflation Algorithm	Pre
View Advanced Options	No
Statistics	
Nodes	127247
Elements	20545
Mesh Metric	None

3.3 Boundary Conditions

The boundary conditions were set with the three different materials assembled. The one basic input is the temperature at which the Bone cement gets to the termination stage of the polymer process; it is, therefore imperative that we determine the effect of that input. The conductive and convective factors are put in place from the prosthesis stem and bone cement respectively.

The outputs needed are the heat flux and the structural effects occurring around the assembly. Hence, a thermostatic analysis was carried out with ambient temperature of 25°C. Since the initiation and termination of the polymerization process of the PMMA polymer is between 40°C and 47°C, extreme boundary condition will occur when the initiation process reaches a peak temperature of 50°C. Here, the heat flux will create several effects thermally and structurally.

3.4 Simulation Studies

The simulation carried out in the present study shows a maximum temperature of 57°C at the bone cement. Maletijt et al. [19], and Yamamato et al. [20], have been clinically testing bioactive bone cement which consists of $CaO\text{-}SiO_2\text{-}P_2O_5\text{-}MgO\text{-}CaF_2$ and that gives maximum temperature of 60°C during polymerisation. The highest surface temperature for PMMA cement composite was 60°C, while that for bioactive bone cement was 35°C. McLaren [1], found the highest temperature to range from 41.4°C to 43.1°C. Peter et al [21], investigated biodegradable bone cement which consisted of PPF (polypropylenefumarate). Its maximum cross-linking temperature was between 38°C and 48°C, which was much lower than the cross-linking temperature of 94°C for PMMA cement [21]. Based on these comparisons, experimental values of temperature obtained in this work can be seen to be within ranges of other temperatures recorded in literature.

With the ambient temperature taken at 25°C for all simulations using Ansys software, the total surface area was found to be $2.95x10^{-6}m^2$.

From the coding of the simulation effect (Fig. 6), it is observed that femur bone received a heat flux of about $1.249x10^{-7}W/m^2$ which emanated from the PMMA bone cement and the heat flux reaching the prosthesis stem was $2.810x10^{-7}$ W/m^2. Although the heat flux may do little or nothing to the femur or prosthesis stem, it should be noted that the heat is also transferred to the blood vessels which might have some effects generally.

The thermal-structural analysis was carried out. The equivalent Von Mises stress, the total deformation, equivalent Von Mises strain and strain energy were determined parametrically within the ranges of loads from the boundary conditions. At 40^oC, the structural effects were observed.

In Fig. 7, the deformation experienced was found to be very small. At the bottom of the assembly, the value was about $4.29x10^{-5}m$. The ends of the assembly experienced the most deformational effect. The centre received the least deformation effect of about $8.65x10^{-7}m$.

From Fig. 8: In terms of the equivalent stress, the femur bone received lower stress of about 2.573MPa from the lower to the upper part of the femur bone while the bone cement and the prosthesis stem received a maximum of 12.39MPa. These stresses are far below the yield strength or ultimate strength of the femur or prosthesis stem but still have some impact on the general assembly.

The strain (Fig. 9) which is the ratio of the elongation to the original length in the x, y and Z coordinates showed a strain of 0.000143m at the femur bone and about 0.000431m at the bone cement. This is also the case in the strain energy as well (Fig. 10). All the results of the simulation studies are summarized in Figs. 11 to 13.

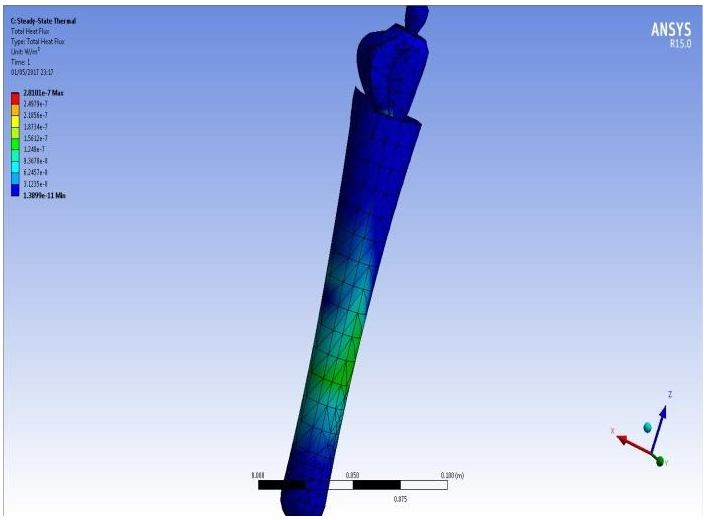

Fig. 6. 40 degrees PMMA Thermal effect

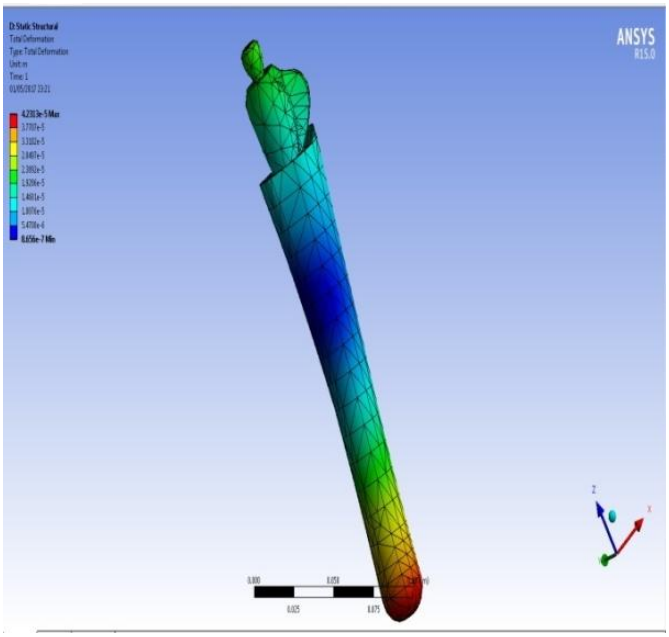

Fig. 7. Total deformation of the Thermo-structural analysis effect

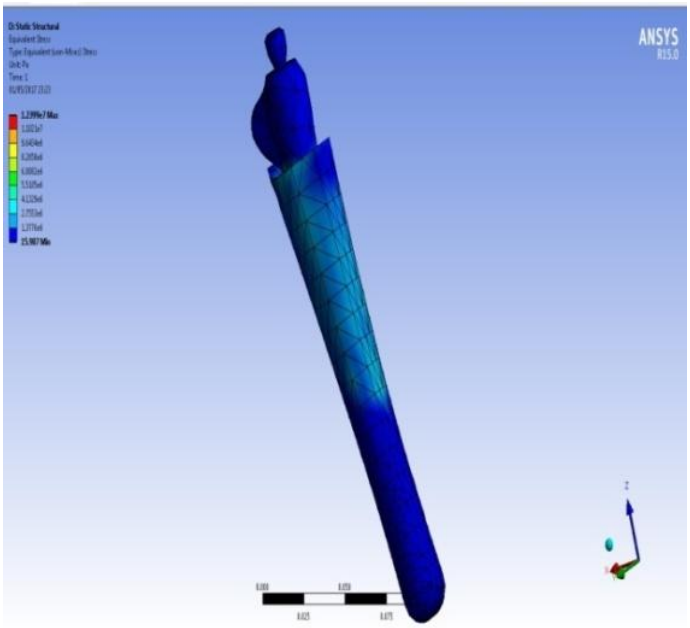

Fig. 8. Equivalent stress of the thermo-structural analysis effect

The heat flux can be seen in both cases to increase with an increasing temperature. It ranged from $1.25x10^{-07}W/m^2$ at 40^oC to $2.83x10^{-07}$ W/m^2 at 50°C for the femur bone, and from $2.81x10^{-07}W/m^2$ at 40°C to $5.11x10^{-07}$ W/m^2 at 50°C for PMMA. The slopes of the graphs (Fig. 11) for both the PMMA and the femur bone gave approximately the specific heat capacities of the two materials respectively: $C_p = \frac{dq}{dT}$. These are given for both the PMMA and Femur bone as: Cp = 1.297kj/kg.^{o}k and Cp = 0.59kj/kg.^{o}k respectively. According to Landgraf et al [22], the specific heat capacity of the PMMA was 1.2kJ/kg.K. This differs from the result of this work by about 7.6%. Fukushima et al [23],

recorded the specific heat capacity of the bone cement (PMMA) as 1.6kJ/kg.K which is about 18% different from the value reported in this work. For the femur bone (cortical bone), Fukushima et al [23], found the specific heat capacity to be 0.46kJ/kg.K which is about 22% different from the result of this work. These percentage differences may be attributable to minor errors in the simulation studies.

The data obtained were fitted to polynomial of the form: $C_p = \alpha + \beta T + \gamma T^2 + \lambda T^3$ to give the temperature dependence of the specific heat capacity of the femur bone as: Cp =$1x10^{-6}$ -$9x10^{-8}$T+$5x10^{-10}$$T^2$+$4X10^{-12}$$T^3$with R^2= 0.9774. For the bone cement, the temperature dependence of the specific heat capacity was found to be: Cp = $3x10^{-7}$+$2x10^{-8}$T-$5x10^{-10}$$T^2$+$4x10^{-12}$$T^3$ with R^2= 0.9926.

The Von Mises stress which is the resultant stress from the three coordinates that describe the failure criteria of the material in question is seen to increase as the temperature increases for both the PMMA cement and the femur. It varied from $2.76x10^{+05}$ Pa at 40°C to$2.14x10^{+06}$ Pa at 50°C for femur and from$1.24x10^{+07}$ Pa at 40°C to$1.93x10^{+06}$ Pa at 50°C for PMMA.

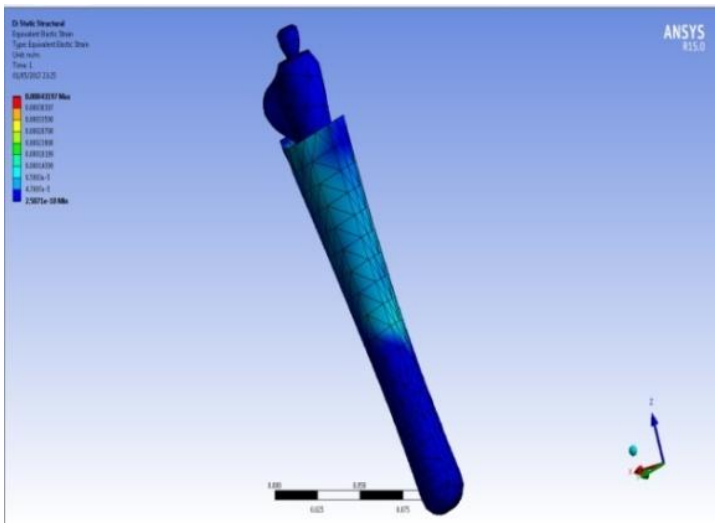

Fig. 9. Equivalent strain of the Thermo-structural analysis effect

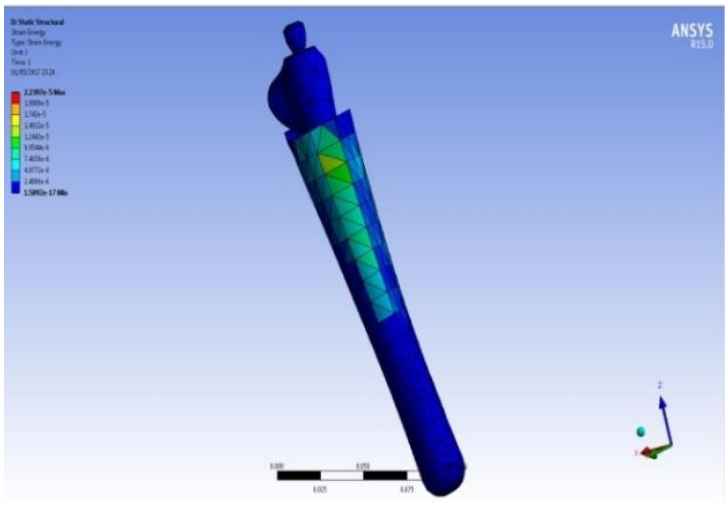

Fig. 10. Strain Energy of the Thermo-structural analysis effect

The strain effect which describes the ratio of the deformation to the original length explains the degree to which a material can be strained beyond its original form. It is seen that the strain increases as the temperature increases for both the PMMA cement and the femur. The young modulus for each of PMMA cement and the Femur was determined from the slope of stress-strain curves of Fig. 12 as 28.78 GPa and 18.79 GPa, respectively.

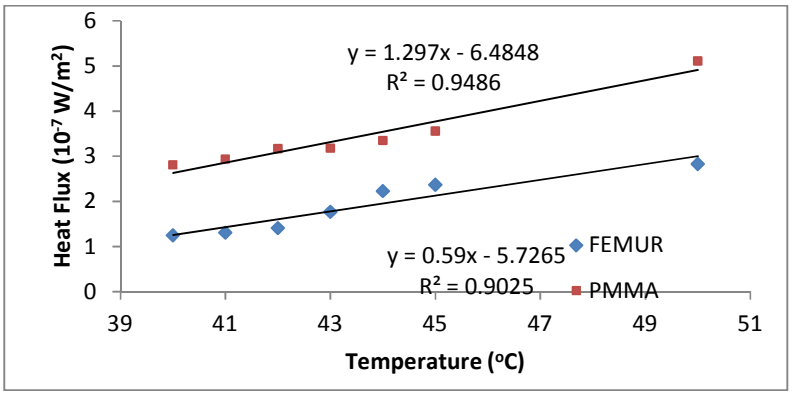

Fig. 11. Heat flux as a function of temperature

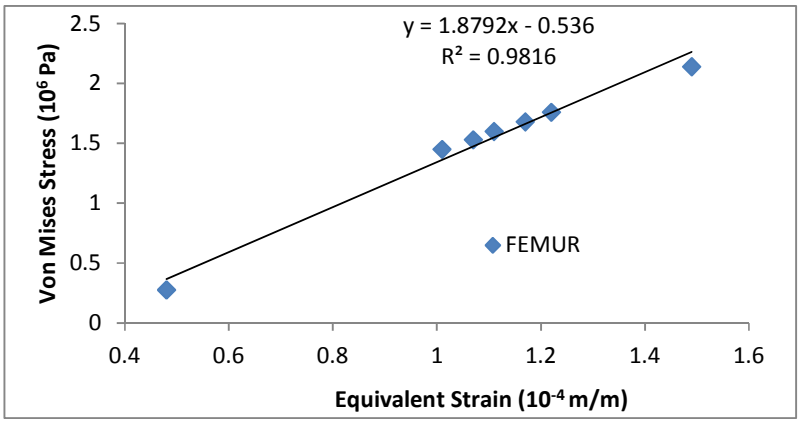

Fig. 12a. Stress–strain relationship: femur bone

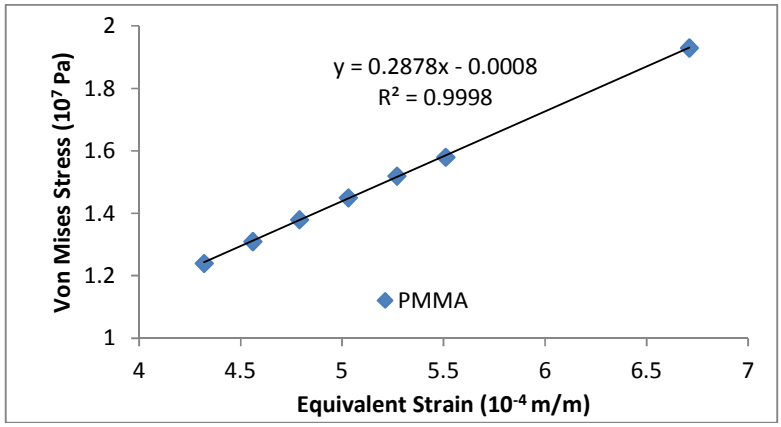

Fig. 12b. Stress-strain relationship for PMMA

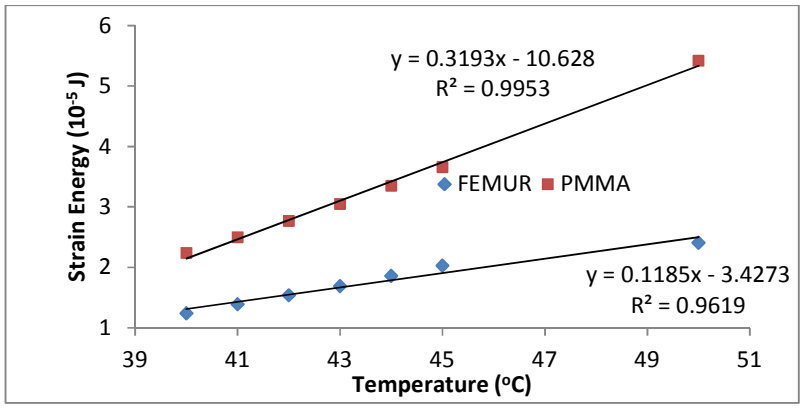

Fig. 13. Strain energy-temperature relation

The Young Modulus for PMMA of 28.78 GPa, is larger than the range of values reported in MIT property database [24]. The differences in the values of Young's Modulus may be due to the fact that the simulation in this work used different cement properties than those used at MIT; they considered pure PMMA while this work considered a combined assemble of the PMMA and the titanium prosthesis stem. The incorporation of titanium, of course, would make the prosthesis stronger, and the fact that the result of this work is far larger is expected.

The Young's Modulus for femur bone of 18.79 GPa is comparable with literature values. Rho et al. [25], using both ultrasonic and micro-tensile measurements found the average trabecular Young's Modulus to be 14.8±1.4 GPa and 10.4±3.5 for bone cement giving an overall average value of 12.6 GPa. This result is smaller than that of this study by about 33%.They found the average Young's Modulus of micro-specimens of cortical bone measured ultrasonically and mechanically as 20.7±1.9 GPa and 18.6±3.5 GPa giving an overall average of 19.65 GPa. This is higher than that of this work by about 4%. The result of this work appears to correlate more with that of micro-specimens of cortical bone determined by the ultrasonic and mechanical tests.

The strain energy is the energy required to strain a material by causing deformations against its original length. We can observe that the strain energies of both the femur bone and the PMMA bone cement increase significantly with an increase in temperature (fig. 13). The strain energy per degree rise in temperature is 0.3193×10^{-5} J/C for PMMA and 0.1185×10^{-5} J/C for the Femur. This shows that the cement is more sensitive to temperature rise than the bone.

4. CONCLUSION

The heat transfer effect in a cemented hip replacement was studied. An experiment was performed to determine the temperature range to be used for simulation. PMMA bone cement preparation involved the mixing of the solid component, powder, with the liquid component in the operating room. That is, the polymerplus the initiator, benzoyl peroxide, and the liquid monomer, Methyl methacrylate (MMA), plus the activator, were mixed. During the polymerization process, monomer MMA was converted into PMMA, which involved an exothermic reaction. The temperature that resulted during this process ranged from 43°C to 47°C. Various literatures reported a temperature ranging from 38oC to 70oC, thus a temperature range of 40 to 50 was used for simulation.

The bone and bone cement thermal and physical properties were obtained from the literature and used to design the femur using ANSYS software. This design exercise properly defined the model geometry, setting the contacts as fixed bonds as there were no moving parts. After this the model was discretized into finite elements, reducing the model into smaller elements with nodes. These elements were defined by fundamental equations and boundary conditions. The meshing process took the tetrahedral elemental structure. The total elements and nodes recorded were 20545 and 127247 respectively. A finite element model of the bone cemented joint was produced using the Computer Aided Engineering (CAE) package, ANSYSv15.0.The increased number of nodes

increased not only the accuracy of the model, but the processing time of the model.

The outputs in the analysis included the heat flux, the deformation, von Mises stress and strain energy as a function of temperature. The simulation gives the total surface area being affected by the increasing temperature as $2.95x10^{-6}m^2$. From the temperature dependence of the heat flux, the specific heat capacities were found to be 1.297kj/kg.^{o}k and 0.59kj/kg.^{o}k respectively for PMMA and Femur bone. Other important findings included the young modulus of the femur of 18.79 GPa and of PMMA as 28.78 GPa.These are comparable with literature values. Other quantities that are affected by the temperature are the deformations, strain and strain energy. It was seen that the temperature that resulted from the exothermic reaction of the PMMA polymer raised the temperature in the assembly creating a heat flux amounting to $5.11x10^{-7}W/m^2$ in which only $2.83x10^{-7}$ W/m^2 got to the femur bone as other has been absorbed by the prosthesis stem and the femur bone. Other effects which were structural might have occurred during this process.

COMPETING INTERESTS

Authors have declared that no competing interests exist.

REFERENCES

1. McLaren AC. Alternative materials to acrylic bone cement for delivery of depot antibiotics in orthopaedic infections. Clinical Orthopaedics and Related Research. 2004;427:101–106.
2. Kweon C, McLaren AC, Leon C, McLeomore R. Amphotericin B Delivery from bone cement increases with porosity but strength decreases. Clinical Orthopaedics and Related Research, 2011;469(11):3002–3007.
3. Vaishya R, Chanhan M, Vaish A. Bone cement. Journal of Clinical Orthopadics and Trauma. 2013;4(4):157–163.
4. Vaishya R, Vaish A, Nadeem A. Bisphosphonate induced atypical subtrochanteric demoral fracture. BMJ Case Report; 2013.
   DOI: 10.11361bcr-2013-201931.
5. Goncalves D, Thompson TJU, Cunha E. Implications of heat-induced changes in bone on the interpretation of funerary behaviour and practice. Journal of Archaeological Science. 2012;38(6):1308 – 1313.
6. Mjˆberg B, Pettersson H, Rosenquist R. Bone cement, thermal injury and the radiolucent zone. Acta Orthopaedica Scand. 1984;55:597–600.
7. Akanksha B, Arjun C, Cila H. Heat transfer model for deep tissue injury: A step towards an early thermographic diagnostic capability. *Diagnostic Pathology.* 2014;9:1 –36.
8. Cengel YA, Ghajar AJ. Heat and mass transfer: Fundamentals & applications. McGraw-Haill Education Pvt Ltd, 5th Ed. 2015;1–879.
9. Tang I – Ming. Finite element method. International Journal of Mechanics. 2011; 5:204.
10. Bergmann G, Graichenn F, Rohlmann A, Verdonschot N, van Lenthe GH. Frictional heating of total hip implants Part 2: finite element study. Journal of Biomechanics. 2001;34:429–435.
11. Baliga BR, Rose PI, Ahmed AM. Thermal modelling of polymerizing considering temperature – distribution heat generation. J Biomech. Eng. 1992; 114:251–259.
12. Perez MA, Nuno N, Madrala A, Garcia-Aznar JM, Doblara M. Computional modelling of bone cement polymerization: temperature and residual stresses. Computers in Biology and Medicine. 2009; 39(9):751–759.
13. Lewis G. Properties of acrylic bone cement: state of the art review. Journal of Biomed. Mater. Res. B (Appl. Biomater.). 1997;38(2):155–182.
14. Wapler MC, Leupold J, Dragonu I, von Elverfeldt D, Zaitsev M, Wallrabe U. Magnetic properties of materials for MR engineering, micro-MR and beyond. JMR. 2014;242:233–242.
   DOI: 10.1016/j.jmr.2014.02.005
15. Pal S. Design of artificial human joints and organs. Springer-Verlag New York Inc., 2014;2014:Ed. 1 – 419.
16. Swenson Jr. LW, Schurman DJ. Finite element temperature analysis of a total hip replacement and measurement of PMMA curing temperature. J Biomed Mater Res. 1981;15.
17. Homsy CA, Tullos HS, Anderson MS. Some physiological aspects of prosthesis stabilization with acrylic polymer. Clinical Orthopaedics and Related Research. 1972;83:317–328.

18. Noble PC. Selection of acrylic bone cements for use in joint replacement. Biomaterials. 1983;4:94–100.
19. Maletijt JDW, Sloof TJJH, Huiskes R. The actual status of acrylic bonecement in total hip replacement. Acta Orthopaedica Belga. 1987;53:52–58.
20. Yamamoto T, Nakamura T, Iida H. Development of bioactive bone cement and its clinical applications. Biomaterials. 1998;19(16):1479–1482.
21. Peter SJ, Kim P, Yasko AW. Crosslinking characteristics of an injectable poly(propylene fumarate)/ β-tricalcium phosphate paste and mechanical properties of the crosslinked composite for use as a biodegradable bone cement. J Biomed Mater Res. 1999;44:314–32.
22. Landgraf R, Ihlemann J, Kolmeder S, Lion A, Lebsack H, Kober C. Modelling and simulation of acrylic bone cement injection and curing within the framework of vertebroplasty. ZAMM - Zeitschrift f¨ur angewandte Mathematik und Mechanik. 2015;1–26.
DOI: 10.1002/zamm.201400064
23. Fukushima H, Hashimoto Y, Yoshiya S, Kurosaka M, Matsuda M, Kawamura S, Iwatsubo T. Conduction analysis of cement interface temperature in total knee arthroplasty. Kobe J. Med. Sci. 2002;48(1 – 2):63–72.
24. MIT (revived 2017), Material Property database.
Available:http://www.io.tudelft.nl/research/dfs/idemat/Onl_db/Id123p.htm
25. Rho JY, Ashman RB, Turner CH. Young's modulus of trabecular and cortical bone material: Ultrasonic and microensile measurements. Journal of Biomech. 1993; 26(2):111–119.

Peer-review history:
The peer review history for this paper can be accessed here:
http://www.sciencedomain.org/review-history/23770